Chinese Chemical Letters 33 (2022) 2555–2558

Contents lists available at ScienceDirect

Chinese Chemical Letters

journal homepage: www.elsevier.com/locate/cclet

Arnequinol A and arnequinone A, two unique meroterpenoids from *Arnebia euchroma*

Hai-Wei Yan, Rong-Rong Du, Xu Zhang, Ya-Nan Yang, Xiang Yuan, Zi-Ming Feng, Jian-Shuang Jiang, Pei-Cheng Zhang*

State Key Laboratory of Bioactive Substance and Function of Natural Medicines, Institute of Materia Medica, Chinese Academy of Medical Sciences and Peking Union Medical College, Beijing 100050, China

ARTICLE INFO

Article history:
Received 22 July 2021
Revised 30 August 2021
Accepted 18 September 2021
Available online 24 September 2021

Keywords:
Arnebia euchroma
Meroterpenoids
Arnequinol A and arnequinone A
Cytotoxicity
Neuroprotective activity

ABSTRACT

Arnequinol A (**1**), featuring an unprecedented 6/6/3 tricyclic carbon skeleton fused with a heptatomic oxo-bridge, together with arnequinone A (**2**) bearing a highly conjugated methyl-shifting benzogeijerene skeleton, were isolated from *Arnebia euchroma*. Their structures were elucidated by extensive spectroscopic methods and quantum chemical calculations of the ^{13}C nuclear magnetic resonance (NMR) data and electronic circular dichroism (ECD) spectra. The plausible biosynthetic pathways for **1** and **2** were presented. In *in vitro* test, compound **2** showed potent neuroprotective activity against serum-deprivation induced PC12 cell damage at a concentration of 10 μmol/L.

The Boraginaceae family, composed of about 130 genera, encompasses about 2700 species, which are distributed in tropical, sub-tropical, and warmer regions world-wide [1,2]. Extensive phytochemical investigations have revealed that some genera of this family, especially *Cordia* [3–5], *Arnebia* [6–8] and *Auxemma* [9,10], presented an abundant source of structurally diverse and biologically active meroterpenoids, consisting of a quinone or hydroquinone linked to a monoterpene motif. The linkage patterns and positions of these two units, and the intramolecular cyclization and rearrangement reactions of the monoterpene moiety provide great potential to the structural diversity of meroterpenoids from this family [4,9,11–13]. To our knowledge, the benzogeijerene skeleton formed by the Cope rearrangement of monoterpene moiety was exclusively found in the Boraginaceae plants [3,14,15].

Arnebia euchroma (Royle) Johnst. belonging to the family Boraginaceae, is a commonly prescribed traditional herbal medicine to treat skin eruption and ulcers, smallpox, jaundice, burn wounds, eczema, and constipation [16]. Up to now, there have been about 40 meroterpenoids reported from *A. euchroma*, of which some compounds displayed potent antiviral, anti-microbial, and cytotoxic activities [13,17–20]. During our further endeavor to discover novel and bioactive meroterpenoids, arnequinol A (**1**) and arnequinone A (**2**) were isolated from the roots of *A. euchroma*. Compound **1** possesses a new 6/6/3 tricyclic carbon skeleton fused with a heptatomic oxo-bridge. And compound **2** bears a novel highly conjugated aromatic system after the 1,2-migration of its tertiary methyl and elimination reaction (Fig. 1). This study describes the isolation, structure elucidation, and proposed biosynthetic pathways of **1** and **2**. The *in vitro* cytotoxic activity of **1**, **1a** (the oxidation product of

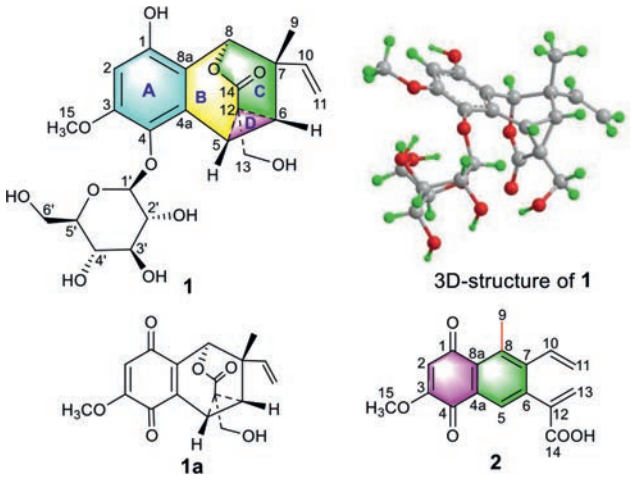

Fig. 1. Chemical structures of **1**, **1a** and **2**.

* Corresponding author.
E-mail address: pczhang@imm.ac.cn (P.-C. Zhang).

https://doi.org/10.1016/j.cclet.2021.09.064
1001-8417/

Table 1
^{1}H (500 MHz) and ^{13}C (125 MHz) NMR data for compounds **1**, **1a**, and **2** (δ in ppm, J in Hz).

Position	**1**[a]		**1a**[b]		**2**[c]	
	δ_C	δ_H	δ_C	δ_H	δ_C	δ_H
1	153.7		184.9	185.7		
2	102.2	6.61, s	107.7	6.08, s	111.5	6.25, s
3	156.0		160.9		158.9	
4	139.4		180.6		179.6	
4a	131.7		140.9		129.5	
5	28.6	3.57, d (7.5)	22.4	3.16, d (7.5)	126.2	7.70, s
6	32.2	2.44, d (7.5)	29.9	2.52, dd (7.5, 2.5)	143.2	
7	37.8		35.5		139.7	
8	78.6	5.46, s	73.4	5.15, d (2.5)	142.0	
8a	113.2		134.8		128.2	
9	23.8	0.88, s	21.4	0.92, s	19.0	2.22, s
10	144.3	6.12, dd (17.5, 11.0)	141.7	6.05, dd (17.5, 11.0)	136.0	7.08, dd (18.0, 11.5)
11a	118.1	5.42, d (17.5)	116.5	5.45, d (17.5)	118.0	5.51, dd (11.5, 1.5)
11b		5.31, d (11.0)		5.28, d (11.0)		5.07, dd (18.0, 1.5)
12	41.0		41.8		141.5	
13	66.7	3.94, d (12.0) 3.89, d (12.0)	62.2	4.02, d (12.0) 3.80, d (12.0)	129.3	6.51, d (1.0) 5.90, d (1.0)
14	176.5		170.3		166.6	
OH-14		-		-		13.07, br s
MeO-15	58.8	3.86, s	57.1	3.86, s	56.5	3.83, s
1′	106.9	4.82, d (7.5)				
2′	76.5	3.62, m				
3′	78.7	3.54, overlap				
4′	72.0	3.54, overlap				
5′	78.8	3.31, m				
6′	63.2	3.77, br s				

[a] Data measured in D_2O.
[b] Data measured in CD_3OD.
[c] Data measured in DMSO-d_6.

the aglycone of **1**) and **2**, as well as neuroprotective activity of **1** and **2** were also evaluated.

Arnequinol A (**1**) was obtained as a white amorphous powder. Its molecule formula $C_{23}H_{28}O_{11}$ with ten indices of hydrogen deficiency was deduced from the high resolution electrospray ionization mass spectroscopy (HRESIMS) sodium adduct ion peak at m/z 503.1521 (calcd. for $C_{23}H_{28}O_{11}Na$, 503.1524). The infrared (IR) absorptions suggested the existence of hydroxyl (3378 cm^{-1}), carbonyl (1698 cm^{-1}), and phenyl (1604, 1505 and 1459 cm^{-1}) functionalities. The ^{1}H nuclear magnetic resonance (NMR) data (Table 1) showed signals for a pentasubstituted benzene ring proton (δ_H 6.61, s), a monosubstituted vinyl [δ_H 6.12 (dd, J = 17.5, 11.0 Hz), 5.42 (d, J = 17.5 Hz), and 5.31 (d, J = 11.0 Hz)], an oxymethine proton (δ_H 5.46, s), an anomeric proton [δ_H 4.82 (d, J = 7.5 Hz)], a hydroxymethyl [δ_H 3.94 (d, J = 12.0 Hz) and 3.89 (d, J = 12.0 Hz)], a methoxy (δ_H 3.86, s), two mutual coupling sp^3 methine protons [δ_H 3.57 (d, J = 7.5 Hz) and 2.44 (d, J = 7.5 Hz)], and a tertiary methyl group (δ_H 0.88, s). Additionally, four oxymethine resonances (δ_H 3.31–3.62, m) and an oxymethylene group (δ_H 3.77, br s) attributable to a glucosyl moiety were observed. The ^{13}C NMR associated with the heteronuclear single quantum coherence (HSQC) spectra assigned 23 carbon signals to an ester carbonyl (δ_C 176.5), a monosubstituted double bond (δ_C 144.3 and 118.1), a phenyl group (δ_C 156.0, 153.7, 139.4, 131.7, 113.2 and 102.2), a glucosyl unit (δ_C 106.9, 78.8, 78.7, 76.5, 72.0 and 63.2), three sp^3 methines involving one oxygenated (δ_C 78.6, 32.2 and 28.6), a hydroxymethyl (δ_C 66.7), a methoxy (δ_C 58.8), a methyl (δ_C 23.8) and two sp^3 nonprotonated carbons (δ_C 41.0 and 37.8). Since a carbonyl, a phenyl, a double bond, and a glucosyl accounted for seven of the ten indices of hydrogen deficiency, the remaining ones required another three rings for **1**.

Interpretation of the ^{1}H-^{1}H COSY spectrum (Fig. 2) indicated two key spin systems, H-5/H-6 and H-10/H$_2$-11. The heteronuclear multiple bond correlation (HMBC) (Fig. 2) correlations from H-2 to C-1, C-3, C-4 and C-8a evidenced the presence of a pentasubstituted benzene ring. The HMBC correlations from H-5 to C-4, C-4a and C-8a, and from H-8 to C-1, C-4a and C-8a established the linkages of C-5 to C-4a and C-8 to C-8a. Meanwhile, MeO-15 and the glucosyl were positioned at C-3 and C-4, respectively, in the light of the HMBC correlations from MeO-15 and H-1′ to the corresponding carbons. Further HMBCs of H-8 with C-6, H-6 with C-8, H-5 with C-7, CH$_3$-9 with C-6, C-7, C-8 and C-10, and H$_2$-11 with C-7 constructed a six-membered carbon ring fused with the benzene ring at C-4a/C-8a and located the monosubstituted double bond and Me-9 at C-7. Moreover, a cyclopropane ring fused to the six-membered carbon ring at C-5 and C-6 was evidenced from the HMBCs of H$_2$-13/C-5, C-6, and C-12, H-5/C-12 and C-13, and H-6/C-5 and C-13. The last degree of unsaturation was furnished with an ester bridge between C-8 and C-12 based on the HMBC correlations from H-5, H-6, H-8, and H$_2$-13 to C-14. Therefore, the planar structure of **1** was unequivocally established (Fig. 1), featuring a unique 6/7/6/3 tetracyclic system.

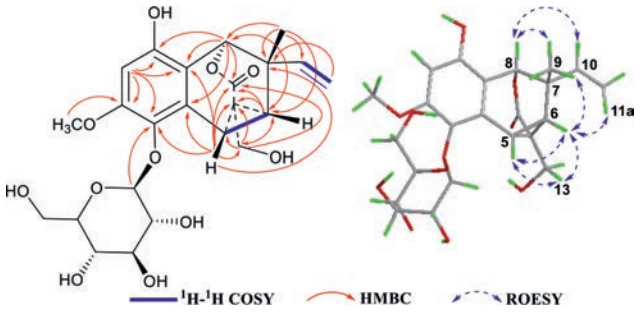

Fig. 2. Key ^{1}H–^{1}H COSY, HMBC and ROESY correlations of **1**.

The β-anomeric configuration of the glucosyl moiety was defined by the coupling constant [δ_H 4.82 (d, J = 7.5 Hz)] of the

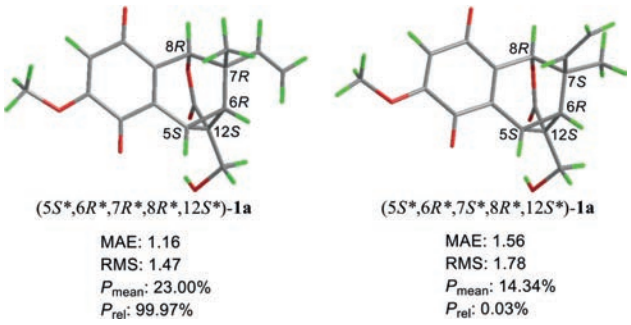

Fig. 3. The ^{13}C NMR chemical shifts calculation results of a pair of C-7 epimers of (5*S**,6*R**,7*R**,8*R**,12*S**)-**1a** and (5*S**,6*R**,7*S**,8*R**,12*S**)-**1a**.

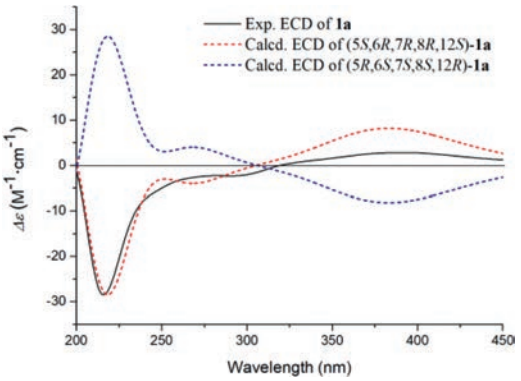

Fig. 4. Experimental ECD and calculated ECD spectra of **1a**.

anomeric proton, and then the D-glucose was ascertained by gas chromatography (GC) analysis [21] (Fig. S2 in Supporting information) after the snailase hydrolysis of **1**. Interestingly, during the hydrolysis process, the aglycone of **1** was autoxidized [22] to its quinone form **1a** (for NMR data, see Table 1). The relative configuration of **1a** was deduced *via* the rotating frame overhauser spectroscopy (ROESY) experiment, conformation analysis, and ^{13}C NMR calculation. The ROESY correlations (Fig. 2) of H-5/H_2-13, H-6/H_2-13, and H-5/H-6 revealed that H-5, H-6, and CH_2-13 were positioned at the same face of the cyclopropane ring. Given the rigidity of the cyclopropane ring and the ester bridge, H-5, H-6, and H-8 must be all in the equatorial orientation (Fig. 2 and Fig. S1 in Supporting information), resulting that the relative configuration at C-7 cannot be resolved though the ROESY correlations of both H-6 and H-8 with Me-9 exist. Hence there are two possible relative configurations for **1a** [(5*S**,6*R**,7*R**,8*R**,12*S**)-**1a** and (5*S**,6*R**,7*S**,8*R**,12*S**)-**1a**, Fig. 3]. The theoretical calculations of ^{13}C NMR chemical shifts of the above two possible isomers were conducted using the GIAO method (Supporting information), following a reported STS protocol [23], which corrected systematic errors according to the types of carbon. As shown in Fig. 3 and Fig. S4 (Supporting information), compared with the experimental data of **1a**, (5*S**,6*R**,7*R**,8*R**,12*S**)-**1a** exhibited smaller mean absolute error (MAE) and root mean square (RMS) values with a P_{rel} probability of 99.97%, defining the relative configuration of **1a** as 5*S**,6*R**,7*R**,8*R**,12*S** with no doubt. Finally, a pair of eligible enantiomers (5*S*,6*R*,7*R*,8*R*,12*S*)-**1a** and (5*R*,6*S*,7*S*,8*S*,12*R*)-**1a** were employed for electronic circular dichroism (ECD) calculations using the time-dependent density functional theory (TDDFT) method at the CAM-B3LYP/6-31+g (d, p) level (Supporting information). The calculated ECD spectrum (Fig. 4) of (5*S*,6*R*,7*R*,8*R*,12*S*)-**1a** matched well with the experimental ECD curve of **1a** allowing the absolute configuration of **1a** determined.

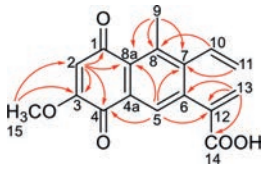

Fig. 5. Key HMBC correlations of **2**.

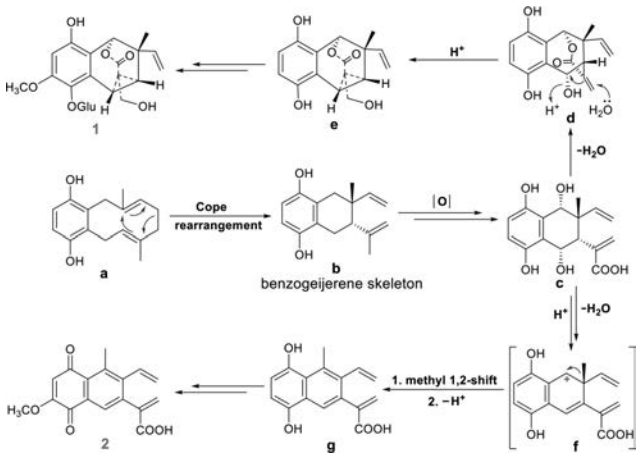

Scheme 1. Proposed biosynthetic pathways of **1** and **2**.

Arnequinone A (**2**), yellowish amorphous powder, had a molecular formula $C_{17}H_{14}O_5$ as determined by the HRESIMS peak at *m/z* 299.0914 $[M + H]^+$ (calcd. for $C_{17}H_{15}O_5$, 299.0914), indicative of eleven degrees of unsaturation. The IR spectrum revealed absorption bands for carbonyl (1682, 1645 cm^{-1}) and phenyl (1615, 1581, 1445 cm^{-1}) groups. The ^1H NMR data (Table 1) displayed signals for an active carboxy hydrogen (δ_H 13.07, br s), a monosubstituted vinyl [δ_H 7.08 (dd, J = 18.0, 11.5 Hz), 5.51 (dd, J = 11.5, 1.5 Hz), and 5.07 (dd, J = 18.0, 1.5 Hz)], a pair of geminal olefinic protons [δ_H 6.51 (d, J = 1.0 Hz) and 5.90 (d, J = 1.0 Hz)], two single aromatic protons [δ_H 7.70 (s) and 6.25 (s)], a methoxy (δ_H 3.83, s), and a methyl (δ_H 2.22, s). The ^{13}C NMR data indicated three carbonyls, twelve sp^2 carbons, a methoxy, and a methyl. All these aromatic carbons represented nine out of eleven degrees of unsaturation, disclosing a dicyclic nucleus for **2**. The key HMBC correlations (Fig. 5) from H-2 to C-1, C-3, C-4 and C-8a, from H-5 to C-4, C-7 and C-8a, and from Me-9 to C-7, C-8 and C-8a constructed the dicyclic nucleus as a 1,4-naphthoquinone with the methyl situated at C-8. Furthermore, HMBCs between H-10 and C-8, between H_2-11 and C-7, between H_2-13 and C-6/C-12/C-14, between H-5 and C-12, and between MeO-15 and C-3 established the linkages of C-7/C-10, and C-6/C-12, and locations of the carboxy and methoxy substituents at C-12 and C-3, respectively. All the above clarified the structure of **2** as a highly conjugated aromatic meroterpenoid with a methyl-shifting benzogeijerene skeleton (Fig. 1) [3,14,15].

Biosynthetically, the key intermediate **b** (Scheme 1) with a benzogeijerene skeleton was yielded *via* a Cope rearrangement of **a** [3,15,24]. Subsequent oxidation and esterification cyclization could generate **d**. Furthermore, intermediate **d** underwent a nucleophilic reaction to produce **e** with the 6/7/6/3 ring system, which would be readily transformed to **1** through selective oxidation methylation and glycosylation. Additionally, the dehydration of intermediate **c**, followed by the subsequent methyl 1,2-shift and elimination reaction generated intermediate **g**, which proceeded oxidation methylation at C-3, cooperated with an autoxidation process to yield compound **2**. Notably, the autoxidation of methoxylated **g** and the aglycone of **1** might be a common feature for 2-methoxyhydroquinones [22].

The cytotoxic activities of **1**, **1a** and **2** against five human tumor cell lines (HCT116, U87-MG, BGC803, HepG2 and PC9) were evaluated using the MTT assay as described in the literature [25]. **1a** exhibited cytotoxicity against all the tested cell lines except HepG2 with the half maximal inhibitory concentration (IC_{50}) values ranging from 19.9 μmol/L to 25.9 μmol/L (Table S3 in Supporting information). Compounds **1** and **2** showed no cytotoxicity ($IC_{50} > 50$ μmol/L, Table S3). Then **1** and **2** were tested for their neuroprotective activities against serum-deprivation induced PC12 cell damage using nerve growth factor (NGF) as the positive control [26]. Compound **2** showed neuroprotective activity with a cell survival rate of 66.50% ± 1.53% compared to that of the model group (51.93% ± 1.36%) at a concentration of 10 μmol/L (Supporting information Table S4).

In conclusion, arnequinol A (**1**) represents an unprecedented 6/6/3 tricyclic carbon skeleton fused with a heptatomic oxo-bridge. Arnequinone A (**2**) bearing a novel highly conjugated aromatic system, was the first example with a methyl-shifting benzogeijerene skeleton in the meroterpenoids from Boraginaceae plants. Their structural novelty could enrich the chemical diversity of meroterpenoids and the chemical constituents of *A. euchroma*.

Declaration of competing interest

The authors declare that they have no known competing financial interests or personal relationships that could have appeared to influence the work reported in this paper.

Acknowledgment

This work was supported by the CAMS Innovation Fund for Medical Sciences (No. 2016-I2M-1-010, China).

Supplementary materials

Supplementary material associated with this article can be found, in the online version, at doi:10.1016/j.cclet.2021.09.064.

References

[1] N. Kumar, R. Kumar, K. Kishore, Pharmacogn. Rev. 7 (2013) 140–151.
[2] R. Gupta, G.D. Gupta, Pharmacogn. Rev. 9 (2015) 127–131.
[3] M. Moir, R.H. Thomson, J. Chem. Soc. Perkin Trans. I. 13 (1973) 1352–1357.
[4] M.J. Oza, Y.A. Kulkarni, J. Pharm. Pharmacol. 69 (2017) 755–789.
[5] T.S. Matos, A.K.O. Silva, A.L. Quintela, et al., Fitoterapia 123 (2017) 65–72.
[6] X.S. Yao, E. Yutaka, N. Hiroshi, et al., Tetrahedron. Lett. 25 (1984) 5541–5542.
[7] A.F. Ahmed, H.A. Saad, E.M.A. El-Karim, Molecules 19 (2014) 5940–5951.
[8] M. Liao, P. Yan, X. Liu, et al., J. Chromatogr. B 1136 (2020) 121924.
[9] O.D.L. Pessoa, T.L.G. Lemos, M.G. Calvalho, et al., Phytochemistry 40 (1995) 1777–1786.
[10] G.M. Costa, T.L.G. Lemos, O.D.L. Pessoa, et al., J. Nat. Prod. 62 (1999) 1044–1045.
[11] S. Dettrakul, S. Surerum, S. Rajviroongit, et al., J. Nat. Prod. 72 (2009) 861–865.
[12] P.P. Painter, B.M. Wong, D.J. Tantillo, Org. Lett. 16 (2014) 4818–4821.
[13] Y. Wang, Y. Zhu, L. Xiao, et al., Fitoterapia 131 (2018) 236–244.
[14] M. Moir, R.H. Thomson, J. Chem. Soc. Perkin Trans. I 15 (1973) 1556–1561.
[15] K. Mori, M. Kawano, H. Fuchino, et al., J. Nat. Prod. 71 (2008) 18–21.
[16] J.M. He, S.C. Sun, Z.L. Sun, et al., Int. J. Antimicrob. Ag. 53 (2019) 70–73.
[17] H.M. Li, Y.L. Tang, Z.H. Zhang, et al., Planta Med. 78 (2012) 39–45.
[18] L. Wang, F. Li, X. Liu, et al., Planta Med. 81 (2015) 320–326.
[19] H. Cao, W. Zhang, D. Liu, et al., Bioorg. Chem. 96 (2020) 103655.
[20] A. Kumar, S. Shashni, P. Kumar, et al., J. Ethnopharmacol. 271 (2021) 113896.
[21] K. Xu, J.S. Jiang, Z.M. Feng, et al., J. Nat. Prod. 79 (2016) 1567–1575.
[22] S. Kim, R. Matsubara, M. Hayashi, J. Org. Chem. 84 (2019) 2997–3003.
[23] J. Li, J.K. Liu, W.X. Wang, J. Org. Chem. 85 (2020) 11350–11358.
[24] G.D. Manners, L. Jurd, J. Chem. Soc. Perkin Trans. I. 4 (1977) 405–410.
[25] Z.F. Hu, A.D. Gu, L. Liang, et al., Green Chem. 21 (2019) 3286–3299.
[26] S.Y. Shao, F. Zhang, Y.N. Yang, et al., Bioorg. Chem. 113 (2021) 105025.